University of Massachusetts, Lowell
Department of Chemical Engineering

Finite Volume Simulation of Acetone Cracking in a Non-Ideal Plug Flow Reactor

Patrick Heng

CHEN 5390

Prof. E.L. Maase

12/09/25

Abstract

Reactive transport phenomena is a fundamental framework for the modeling of chemical reactors. While these models have a strong theoretical basis, the resulting partial differential equations that describe the phenomena are highly non-linear and have significant coupling between each other. This leads to 'stiff' differential equations that are expensive or unstable to integrate, even for relatively simple reactions. In the following, we explore a finite volume based solver for 1D problems and develop an algorithm to iteratively solve the Concentration, U momentum, and Temperature (CUT) equations. As a case study, we further develop a model for a plug flow reactor with axial dispersion and test the solver with conditions simulating the thermal cracking of acetone. This reaction has a highly temperature dependent rate constant and thus serves as a reasonable benchmark to test the performance of the CUT algorithm in a moderately non-linear setting.

Contents

Table 1: Nomenclature

Symbol	Denotes	Units (SI)
c_i	Concentration of species i	$\mathrm{mol} \cdot \mathrm{m}^{-3}$
M_i	Molar mass of species i	$\mathrm{mol} \cdot \mathrm{kg}^{-1}$
ν_i	Stoichiometric coefficient of species i	1
$C_{p,i} = a_0 + a_1 T + a_2 T^2$	Molar heat capacity of species i	$\mathrm{J} \cdot \mathrm{mol}^{-1} \cdot \mathrm{K}^{-1}$
r_i	Total reaction rate of species i	$\mathrm{mol} \cdot \mathrm{m}^{-3} \cdot \mathrm{s}^{-1}$
u	Axial flow velocity	$\mathrm{m} \cdot \mathrm{s}^{-1}$
T	Absolute temperature	K
p	Absolute pressure	$\mathrm{J} \cdot \mathrm{m}^{-3}$
$\hat{\rho} = \sum_i c_i M_i$	Mixture density	$\mathrm{kg} \cdot \mathrm{m}^{-3}$
$\hat{H} = \sum_i T c_i C_{p,i}(T)$	Mixture enthalpy	$\mathrm{J} \cdot \mathrm{mol}^{-1} \cdot \mathrm{K}^{-1}$
ΔH°_{rxn}	Molar reaction enthalpy at reference temperature	$\mathrm{J} \cdot \mathrm{mol}^{-1}$
$K = c_{A,0} \sum_i \Theta_i C_{p,i}(T_0)$	Initial volumetric heat capacity	$\mathrm{J} \cdot \mathrm{m}^{-3}$
D	Axial dispersion coefficient	$\mathrm{m}^2 \cdot \mathrm{s}^{-1}$
μ	Average mixture viscosity	$\mathrm{kg} \cdot \mathrm{m}^{-1} \cdot \mathrm{s}^{-1}$
κ	Average mixture thermal conductivity	$\mathrm{J} \cdot \mathrm{m}^{-1} \cdot \mathrm{s} \cdot \mathrm{K}^{-1}$
T_a	Heat exchanger temperature	K
T_{ref}	Thermodynamic reference temperature	K
E_a	Reaction activation energy	$\mathrm{J} \cdot \mathrm{mol}^{-1}$
k_0	Arrhenius frequency factor	s^{-1}
R	Universal gas constant	$\mathrm{J} \cdot \mathrm{mol}^{-1} \cdot \mathrm{K}^{-1}$
$\hat{q}_{rxn}$	Heat of reaction	$\mathrm{J} \cdot \mathrm{m}^{-3} \cdot \mathrm{s}^{-1}$
$\hat{q}_{ext}$	Heat exchanger heating rate	$\mathrm{J} \cdot \mathrm{m}^{-3} \cdot \mathrm{s}^{-1}$
h	Heat transfer coefficient	$\mathrm{J} \cdot \mathrm{m}^{-2} \cdot \mathrm{s}^{-1}$
A	Inner reactor surface area	m^2
V	Inner reactor volume	m^3
x	Distance from reactor entrance	m
L	Total reactor length	m

Table 2: Dimensionless Groups

Symbol	Expression	Denotes
C_A	$\frac{c_A}{c_{A,0}}$	Normalized concentration of A
U	$\frac{u}{U_0}$	Normalized velocity
θ	$\frac{T}{T_0}$	Normalized temperature
H	$\frac{\hat{H}}{K}$	Normalized enthalpy
P	$\frac{p}{p_0}$	Normalized pressure
ρ	$\frac{\hat{\rho}}{\rho_0}$	Normalized density
X	$1 - C_A U$	Conversion of A
β	$\frac{-E_a}{RT_0}$	Normalized activation energy
Θ_i	$\frac{c_{i,0}}{c_{A,0}}$	Normalized initial concentration of species i
Pe_M	$\frac{U_0 L}{D}$	Mass Pèlcet number
Pe_T	$\frac{U_0 L K}{\kappa}$	Thermal Pèlcet number
Re	$\frac{\rho_0 U_0 L}{\mu}$	Reynolds number
Eu	$\frac{p_0}{\rho_0 U_0^2}$	Euler number
Da	$\frac{k_0 L}{U_0}$	Damköhler Number
Γ	$\frac{c_{A,0}}{KT_0}\left(\Delta H^{\circ}_{rxn} - \sum_i \nu_i \int_0^{T_{ref}} C_{p,i}\, dT\right)$	Normalized reference enthalpy
q_{rxn}	$-Da\, e^{\beta/\theta} C_A \left(\Gamma + \frac{c_{A,0}}{KT_0} \sum_i \nu_i \int_0^{T} C_{p,i}\, dT\right)$	Normalized heat of reaction
q_{ext}	$\frac{hAL}{VKU_0}\left(\frac{T_a}{T_0} - \theta\right)$	Normalized heat exchange rate
z	$\frac{x}{L}$	Normalized distance

* Subscript 0's denote the variable evaluated at the inlet conditions

PFR Model & Governing Equations[1]

Consider a decomposition reaction of A, which forms products, B and C,

$$aA \rightarrow bB + cC, \tag{1}$$

where a, b, and c are the stoichiometric coefficients of the reaction. This reaction can be carried out in a 'plug flow reactor' (PFR) where the fluid reactant is passed through a tube with elevated pressure and temperature to drive the reaction [1].

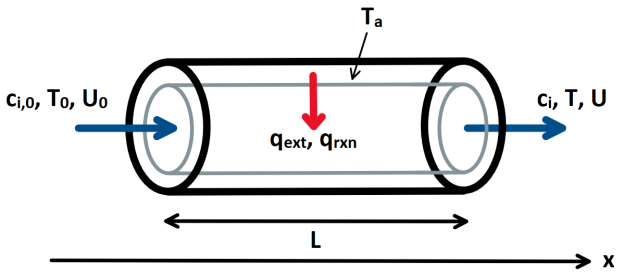

Figure 1: Diagram of plug flow reactor with a shell and tube heat exchanger operating with an outside fluid temperature of T_a. At the inlet, c_i, T, and U are known and specified as Dirichlet boundary conditions. At the outlet, the c_i, T, and U profiles remain undisturbed by the exit, so a no-flux (Neumann) condition is imposed.

A specific example that will be considered to validate the developed numerical method is the thermal cracking of acetone (CH_3COCH_3, A) which is inspired by the problem given in [2]. This reaction produces ketene (CH_2CO, B) which is a precursor to acetic anhydride, an important reactant in organic synthesis. In absence of a catalyst, this is a homogeneous gas phase reaction,

$$CH_3COCH_3 \rightarrow CH_2CO + CH_4, \tag{2}$$

which follows first order reaction kinetics. To simplify the analysis of the reactor, it will be assumed there are no radial or angular variation of all variables and only consider variation along the x axis. Conservation of mass, momentum, and energy, gives the following equations [2] [3],

$$\frac{\partial c_A}{\partial t} + \frac{\partial \left(u c_A\right)}{\partial x} = D\frac{\partial^2 c_A}{\partial x^2} + r_A, \tag{3}$$

$$\frac{\partial \left(\hat{\rho} u\right)}{\partial t} + \frac{\partial \left(\hat{\rho} u u\right)}{\partial x} = \mu\frac{\partial^2 u}{\partial x^2} - \frac{\partial p}{\partial x}, \tag{4}$$

$$\frac{\partial \hat{H}}{\partial t} + \frac{\partial (U\hat{H})}{\partial x} = \kappa\frac{\partial^2 T}{\partial x^2} + \hat{q}_{rxn} + \hat{q}_{ext} + \frac{\partial p}{\partial t} + u\frac{\partial p}{\partial x}. \tag{5}$$

[1] This section is taken directly from the original report given in MECH 5200, but is provided here for background on the problem.

[2] Physically, the diffusion term in each of the equations is small and could be neglected, but they are maintained for numerical stability. Diffusion makes the resulting matrices more diagonally dominant and more suitable to perform iterative methods.

where the main solution variables are the concentration of A, c_A, the fluid velocity, u, and the fluid temperature, T. It is assumed that the axial dispersion coefficient, D, viscosity, μ, and thermal conductivity, κ, are constant and the same for all chemical species. r_A is a reaction term of the form,

$$-\frac{r_A}{a} = k_0 \exp\left(\frac{-E_a}{RT}\right) c_A^{\alpha}, \tag{6}$$

where $\alpha = 1$ for our specific reaction. The volumetric heat released by the reaction, $\hat{q}_{rxn}$, may be modeled by the reaction rate times the reaction enthalpy,

$$\hat{q}_{rxn} = k_0 \exp\left(\frac{-E_a}{RT}\right) c_A^{\alpha} \left(\Delta H^{\circ}_{rxn} - \sum_i \nu_i \int_0^{T_{ref}} C_{p,i}\, dT + \sum_i \nu_i \int_0^{T} C_{p,i} dT\right), \tag{7}$$

where the heat capacities, $C_{p,i}$, are further given by empirical polynomials [5],

$$C_{p,i}(T) = \left(a_0 + a_1 T + a_2 T^2\right)_i. \tag{8}$$

Finally, the external heating rate, $\hat{q}_{ext}$, may be modeled with a constant ambient temperature heat exchanger,

$$\hat{q}_{ext} = \frac{hA}{V}\left(T_a - T\right), \tag{9}$$

where h is the heat transfer coefficient, A is the heat transfer area, V is the reactor volume, and T_a is the heat exchanger temperature. For computational purposes, it is convenient to non-dimensionalize the governing equations,

$$\frac{\partial C_A}{\partial t} + \frac{\partial\left(UC_A\right)}{\partial z} = \frac{1}{Pe_M}\frac{\partial^2 C_A}{\partial z^2} - Da\, e^{\beta/\theta} C_A, \tag{10}$$

$$\frac{\partial\left(\rho U\right)}{\partial t} + \frac{\partial\left(\rho U U\right)}{\partial z} = \frac{1}{Re}\frac{\partial^2 U}{\partial z^2} - Eu\frac{\partial P}{\partial z}, \tag{11}$$

$$\frac{\partial H}{\partial t} + \frac{\partial\left(UH\right)}{\partial z} = \frac{1}{Pe_T}\frac{\partial^2 \theta}{\partial z^2} + q_{rxn} + q_{ext} + \frac{p_0}{KT_0}\left(\frac{\partial P}{\partial t} + U\frac{\partial P}{\partial z}\right), \tag{12}$$

where the dimensionless variables are defined in the 'Dimensionless Groups' table. While the governing PDE's have been derived for the problem, an equation of state must be supplied to solve for the pressure in the reactor. An ideal gas assumption is *not* valid at the operating conditions, however, the dimensionless *ratio* between the inlet and outlet states is approximately ideal for small variations in p and T [1]. With this assumption, the following relations hold,

$$P = \frac{\left(1 + \varepsilon X\right)\theta}{U}, \tag{13}$$

$$\rho = \frac{c_{A,0}}{\rho_0}\frac{\sum_i \left(\Theta_i M_i + (\nu_i/a) X M_i\right)}{1 + \varepsilon X}\left(\frac{P}{\theta}\right), \tag{14}$$

$$H = \frac{c_{A,0}}{K}\sum_i \left[\left(\Theta_i - \frac{\nu_i}{a}X\right) C_{p,i}\right]\left(\frac{\theta}{U}\right), \tag{15}$$

where,

$$X = 1 - UC_A, \tag{16}$$

is the conversion of A, and,

$$\varepsilon = -\frac{1}{a}\frac{\sum_i \nu_i}{\sum_i \Theta_i}, \tag{17}$$

is related to the change in moles due to the reaction.

Objectives of the Present Project

The original project was able to develop a steady state solver for the system of PDE's, but the transient solver was neglected due to time constraints. Therefore, the main objective of the current project is to develop a time integration scheme to model a step input to the concentration of the reactor. Additionally, the original model assumed that the ambient temperature for the heat exchanger was constant, which is not necessarily realistic since the reaction is extremely endothermic and requires a lot of heat input. To improve upon the original model, the objectives of this project are presented in the following list.

- Implement a transient solver for the PDE system
  - Improve the momentum equation for more realistic/stable solutions
  - Implement flux limiters in the finite volume scheme for stability
- Model the spatial and temporal variations of the heat exchange fluid surrounding the PFR
- Develop a control law to control the temperature of the reactor by manipulating the heating fluid flow rate
  - Test various controller gains and observe the response time and magnitude of the control input
  - Test controller for various inlet concentrations

Improvements to the Original Model

Implementation of the Transient Solver

The PDE system from a finite volume discretization can be generally stated in the following way,

$$\frac{d\mathbf{y}}{dt} = \mathbf{F}\left(t, \mathbf{y}\right), \tag{18}$$

where $\mathbf{y}$ is the vector of all unknowns (C_A, U, θ at all nodes) and $\mathbf{F}$ is the nonlinear function resulting from the discretization. The original model solved the steady problem, i.e.,

$$\mathbf{0} = \mathbf{F}\left(t, \mathbf{y}\right), \tag{19}$$

which is solved iteratively by a Newton or fixed-point solver. In theory, implementation of a time integration scheme for the system of PDE's could be as simple as using a forward Euler approximation,

$$\frac{\mathbf{y}^{k+1}-\mathbf{y}^{k}}{\Delta t}=\mathbf{F}\left(t,\mathbf{y}^{k}\right)=\mathbf{F}^{k}, \tag{20}$$

where k is the time step and Δt is the step size. In practice, this scheme is unstable for practical time steps in parabolic systems [4,10]. A more subtle approach is the use an implicit Euler scheme,

$$\frac{\mathbf{y}^{k+1}-\mathbf{y}^{k}}{\Delta t}=\mathbf{F}^{k+1}, \tag{21}$$

which requires the solution to a nonlinear system of algebraic equations. The main attraction with an implicit scheme is that it is unconditionally stable for all time steps [4,10], meaning that the numerical solution will always track the actual solution for all time. This does *not* mean the system itself is stable and the solution can still diverge.

This leads the next concern which is that the spatial discretization can affect the stability of the simulation. For example, it is known that a second order central difference for the first derivative causes nonphysical oscillations in the numerical solution. In fact, it is generally true that without the use of 'flux limiters', any spacial discretization higher than first order will cause oscillations (Godunov's Theorem [10]). Flux limiters are the solution to this problem, which restrict how large the gradient in a solution is and preserves the hyperbolic nature of the solution. For the concentration equation, this amounts to using the following modification to the dicretization,

$$\frac{d\bar{C}_{A,i}}{dt}+(1-\phi_i)\left[\frac{\bar{U}_i\bar{C}_{A,i}-\bar{U}_{i-1}\bar{C}_{A,i-1}}{\Delta z}\right]+\phi_i\left[\frac{\bar{U}_{i+1}\bar{C}_{A,i+1}-\bar{U}_{i-1}\bar{C}_{A,i-1}}{2\Delta z}\right]=\cdots, \tag{22}$$

where $\phi_i(r_i)$ is the flux limiter, and r_i is defined by,

$$r_i=\frac{\bar{C}_{A,i}-\bar{C}_{A,i-1}}{\bar{C}_{A,i+1}-\bar{C}_{A,i}}. \tag{23}$$

The ϕ_i term is essentially just a weighted average of a first and second order discretization. When the solution has small gradients, ϕ_i is close to 1, and the higher order central difference scheme is used. In contrast, when there are large gradients, ϕ_i is close to 0 and first order scheme is used to preserve stability. There are many choices for ϕ_i, but the one chosen for this solver was the 'minmod' limiter [10],

$$\phi_i(r_i)=\max\left(0,\min\left(1,r_i\right)\right), \tag{24}$$

which is generally more stable, but can lead to some numerical diffusion. These modifications are necessary since inputting a step change to the reactor entrance conditions produces a discontinuity in the transport fields. Therefore, the transport gradients need to be limited in these regions to keep the solver stable. Other than these modifications, the transient solver is similar to the steady solver. The main difference is that the algebraic equation to solve is,

$$\frac{\mathbf{y}^{k+1}}{\Delta t}-\mathbf{F}^{k+1}=\frac{\mathbf{y}^{k}}{\Delta t}, \tag{25}$$

where the left hand size is just another nonlinear function and the $\mathbf{y}^k/\Delta t$ term acts as a forcing function.

Improved Pressure Drop Model

The original model solved for the pressure field, P, via an ideal gas approximation. However, this led unrealistic solutions to the velocity field as the velocity increased along the length of the reactor. This problematic since the the density increases due to the reaction, meaning the velocity should decrease to conserve momentum. As a better approximation to the pressure gradients within the PFR, the nondimensionalized Darcy-Weisbach equation can be used [1],

$$\frac{\partial P}{\partial z} = f\left(\frac{L}{D}\right)\frac{1}{2}\rho U^2, \tag{26}$$

where, f is the Darcy friction factor and D is the hydraulic diameter. Alternatively, for a packed-bed reactor, the Ergun equation can be used [1]. As first approximation, the friction factor is calculated from the Colebrook-White equation [1], based on the initial conditions in the reactor,

$$\frac{1}{\sqrt{f}} = -2\log\left(\frac{e}{3.7D} + \frac{2.51}{Re\sqrt{f}}\right), \tag{27}$$

where e is the pipe roughness (assumed equal to 5e-5 m for steel piping) and Re is the Reynolds number based on the reactor diameter. f will be assumed constant throughout the pipe to simplify calculations. While this pressure drop equation can be plugged directly into the momentum equation, this led to unstable solutions. The main complication can be attributed to the time derivative term in the momentum equation. This is because the pressure time scale is much faster than convective time scale, meaning that the pressure wave can only be resolved if the time step it taken extremely small. This issue was resolved by completely removing the time derivative term in the momentum equation, which physically means that the pressure wave travels instantaneously. This means the momentum field only changes due to changes in the temperature and does not directly depend on time. Mathematically, the dimensionless momentum equation satisfies,

$$\frac{\partial\left(\rho U U\right)}{\partial z} = \frac{1}{Re}\frac{\partial^2 U}{\partial z^2} - f\left(\frac{L}{D}\right)\frac{1}{2}\rho U^2, \tag{28}$$

which can be discretized in a similar manner to the other equations and is discussed further in the following section.

Heating Fluid Energy Balance

Due to the high temperature required, this reaction would often take place in a furnace, which is mathematically hard to model. Thus, for simplicity, it is assumed that the flue gas from the furnace runs countercurrent in a heating jacket around the reactor tubes. Additionally, the heat capacity and density of the flue gas is assumed constant to simplify the model. By performing an energy balance on a Δx sized slice of the flue gas,

$$[\text{Accumulation}] + [\text{Convection (Flux in} - \text{Flux out)}] = [\text{Generation}], \tag{29}$$

$$A\Delta x\frac{\partial\left(\rho C_p T_a\right)}{\partial t} + \dot{m}C_p\left(T_{a,x+\Delta x} - T_{a,x}\right) = -A\Delta x\left[\frac{hA}{V}\right]\left(T_a - T\right), \tag{30}$$

where $\dot{m}$ is the mass flow of the flue gas, ρ is the gas density, C_p is the specific heat capacity of the flue gas, A is reactor cross sectional area, hA/V is the heat transfer per unit volume $[\mathrm{W/m^3 \cdot K}]$, and T is the reactor temperature. Assuming ρC_p is constant, dividing the entire equation by $(A\Delta x)(\rho C_p)$, and taking the limit as $\Delta x \to 0$ gives the following energy balance for the flue gas,

$$\frac{\partial T_a}{\partial t} + \frac{\dot{m}}{\rho A}\frac{\partial T_a}{\partial x} = -\frac{1}{\rho C_p}\frac{hA}{V}\left(T_a - T\right). \tag{31}$$

This can be non-dimensionalized by making the following substitutions,

$$\theta_a = T_a/T_{a,0}, \quad z = x/L, \quad t \to U_0 t/L, \tag{32}$$

which gives,

$$\frac{\partial \theta_a}{\partial t} + \left[\frac{\dot{m}}{\rho A U_0}\right]\frac{\partial \theta_a}{\partial z} = -\left[\frac{hAL}{\rho C_p V U_0}\right]\left[\theta_a - \theta\left(\frac{T_0}{T_{a,0}}\right)\right]. \tag{33}$$

The outlet boundary condition is a no flux condition, which allows the fluid to naturally exit. The entry condition is simply a specified (Dirichlet) temperature. Mathematically,

$$\frac{\partial \theta_a}{\partial z} = 0 \text{ at } z = 0 \quad \text{and} \quad \theta_a = 1 \text{ at } z = 1. \tag{34}$$

The equation can be solved numerically by performing a finite volume discretization. This gives following algebraic relation for the first derivative,

$$\left(\frac{\partial \theta_a}{\partial z}\right)_i = (1-\phi_i)\left[\frac{\theta_{a,i} - \theta_{a,i-1}}{\Delta z}\right] + \phi_i\left[\frac{\theta_{a,i+1} - \theta_{a,i-1}}{2\Delta z}\right], \tag{35}$$

where ϕ_i the minmod flux limiter (Eq. 24), which is a function of r_i,

$$r_i = \frac{\theta_{a,i} - \theta_{a,i-1}}{\theta_{a,i+1} - \theta_{a,i}}. \tag{36}$$

Thus, by plugging this into the PDE with an implicit time integration scheme,

$$\begin{aligned}\frac{\theta_{a,i}^{k+1} - \theta_{a,i}^{k}}{\Delta t} + \left(1-\phi_i^k\right)\left[\frac{\dot{m}}{\rho A U_0}\right]\left[\frac{\theta_{a,i}^{k+1} - \theta_{a,i-1}^{k+1}}{\Delta z}\right] + \phi_i^k\left[\frac{\dot{m}}{\rho A U_0}\right]\left[\frac{\theta_{a,i+1}^{k+1} - \theta_{a,i-1}^{k+1}}{2\Delta z}\right] \\ = \left[\frac{hAL}{\rho C_p V U_0}\right]\left[\theta_a^{k+1} - \theta^{k+1}\left(\frac{T_0}{T_{a,0}}\right)\right].\end{aligned} \tag{37}$$

This is another nonlinear algebraic system for the $\theta_{a,i}^{k+1}$ unknowns. This can be solved in an equation tearing approach, meaning that θ_a solved for after C_A, U, and θ have already been solved for.

Temperature Controller Model

As a final exploration, a simple (naive) control law was developed to choose an appropriate flue gas flow rate, $\dot{m}$, to use. The main complication with PFR control is that often, the

interior temperature cannot be measured, and must be inferred from the inlet conditions and a predictive model. This is a large motivation for why some PFR's are run adiabatically with interstage cooling or heating, as it is simpler to control. However, for the sake of exploration, the developed model will be used to synthesize a control law for the countercurrent PFR.

In theory, the controller would solve the PDE system at every time step to choose a new $\dot{m}$ value to use. With this, the proposed control law is given as follows,

$$\dot{m}^{k+1} = \int_0^1 K_c \left[\left(\frac{T^{k+1} - T_a^{k+1}}{T_{a,0}} \right)^2 + \lambda \left(\frac{T^{k+1}}{T_0} - 1 \right)^2 \right] dz, \tag{38}$$

where K_c is the controller gain and λ is a constant. The motivation for this law is that the first term measures the average squared deviation of the reactor temperature, T, from the heat jacket temperature, T_a. If the temperature difference is small across the entire reactor, the flow rate will also be small, and the opposite is true if the difference is large. In practice, $\dot{m}$ is capped by a certain value, say 10 kg/s, to limit the control action. The λ term penalizes any difference between the reactor temperature from the inlet temperature, because ideally, these values should be close. Larger λ values should make the flow rate high enough such that temperature crossover in the heat exchanger does not occur or is limited. The optimal K_c and λ values can be theoretically derived by optimal control theory [11] since the $\dot{m}$ term is essentially a cost function for which minimal K_c and λ values exist. However, for simplicity, the values of K_c and λ were simply guessed until reasonable solutions were achieved.

Developed MATLAB Scripts

Since this project was based on an existing code, any additions to the code are denoted by a line of '+++' comments encasing any new code lines. Most of the .m files only contained minor changes to add the transient solver and flux limiters. However, the major additions came in the the following files.

- PFR_FV_test_CUT_transient.m (Main driver script)
- PFR_transient_plots.m (Script to plot the dynamics of system once main driver is run)
- stencil_coefficients_Ta.m (Sets up algebraic equations for θ_a)
- stencil_coefficients_U.m (Sets up algebraic equations for U)

Minor additions were added to the following files.

- stencil_coefficients_CA.m (Sets up algebraic equations for C_A)
- stencil_coefficients_theta.m (Sets up algebraic equations for θ)

While there are many lines of code, the basic principle of the solver is the same as the nonlinear BVP problems solved in class. At each time step (outer loop), a nonlinear system is solved by linearizing the system for each transport field until the 'inner loop' of linear systems converges to the nonlinear solution. This is repeated until the desired simulation time is reached.

Results & Validation

The results were simulated using the parameters given in the following table.

Table 3: PFR simulation parameters

Parameter	Value
Initial acetone concentration (mol/m^3)	16.92
Initial product concentration (mol/m^3)	0
Inlet reactor temperature (K)	1000
Inlet HX temperature (K)	1150
Reactor length (m)	4
Shell diameter (m)	1
Tube diameter (m)	0.0266
Number of tubes (·)	1000
Pipe roughness (m)	5E-05
Inlet reactor velocity (m/s)	4
Mixture thermal conductivity (J/m-K)	0.2
Mixture mixing coefficient (m^2/s)	0.01
Mixture viscosity (kg/m-s)	3E-05
Heat transfer coefficient (J/m^{2-}s-K)	110
Flue gas density (kg/m^3)	1.175
Flue gas heat capacity (J/kg-K)	1159

The data is from the problem given in [1], which based a PFR with 1000 1 inch schedule 40 pipes encased by a shell containing the heating gas. Additionally, molecular weights and polynomial heat capacity coefficients were taken from [5] and the exact values may be seen in the main script.

Numerically, 100 nodes were used in the discretization and it was validated in the previous project that the numerical solver becomes more accurate as the number of nodes increases. The time step size was determined by the CFL condition [10],

$$\Delta t = \frac{\Delta x}{U_0}, \tag{39}$$

where U_0 is the inlet velocity, and Δx is the physical grid spacing. Physically, this time step is chosen since information cannot propagate faster than the fluid speed, U_0, which sets the limit on Δt.

Steady State Solution - Model Validation

Although the main objective of the project is to implement a transient solver, a steady state solution should still be achieved for long times. As an initial test, the solver was set to 300 time steps to arrive at a steady solution. Originally, the model was going to be validated against a COMSOL dynamic model, but time constraints prevented this. Instead, the steady solution will be compared to a PFR model given in Aspen Plus. In Aspen Plus, the heating

jacket temperature was set to a constant 1150 K since it does not support a countercurrent heater design. The MATLAB solver can be set to a constant temperature by setting K_c to a very large number so that the flue gas flow rate is essentially infinite. The following figure show the steady solution for both solvers, displaying the mole fraction, temperature and reaction rate fields.

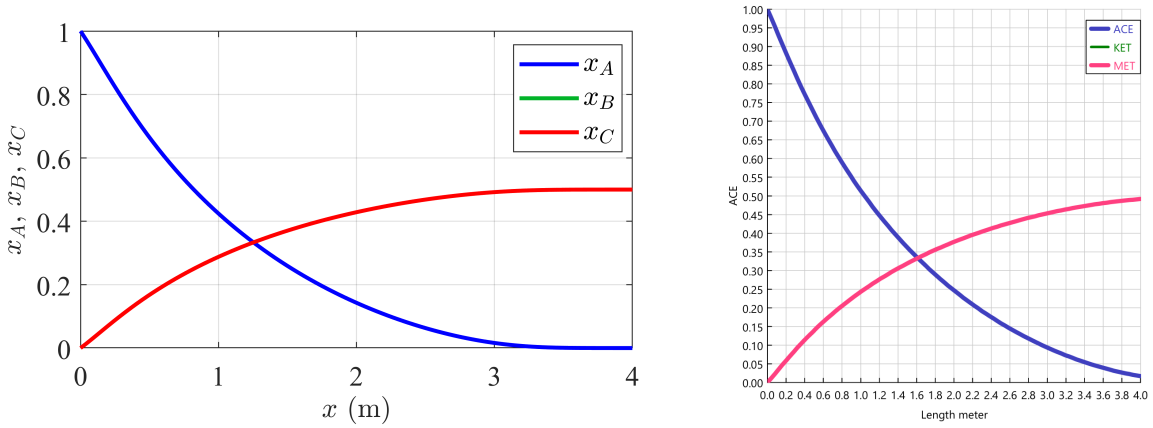

Figure 2: [Left] MATLAB steady mole fraction profile in PFR (A: Acetone, B: Ketene, C: Methane); [Right] Aspen Plus steady mole fraction profile in PFR

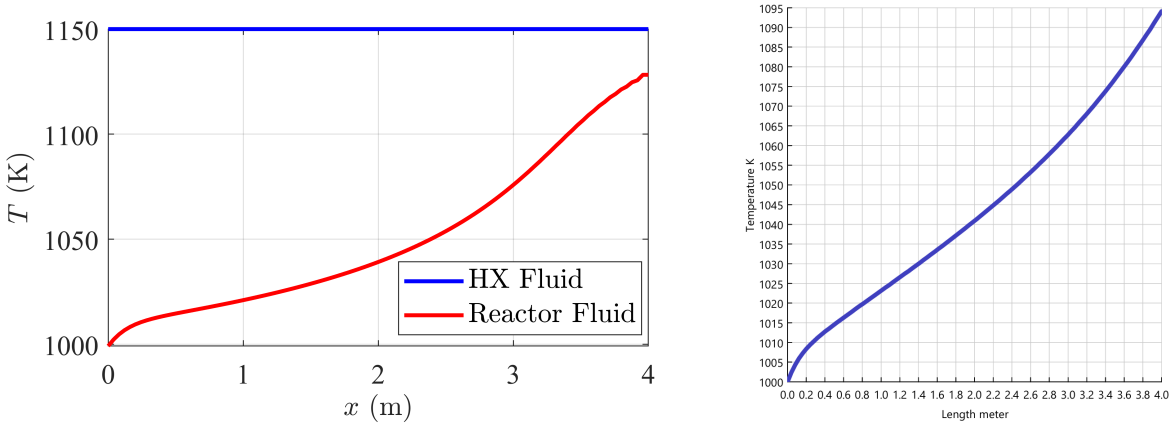

Figure 3: [Left] MATLAB steady temperature profile in PFR; [Right] Aspen Plus steady temperature profile in PFR

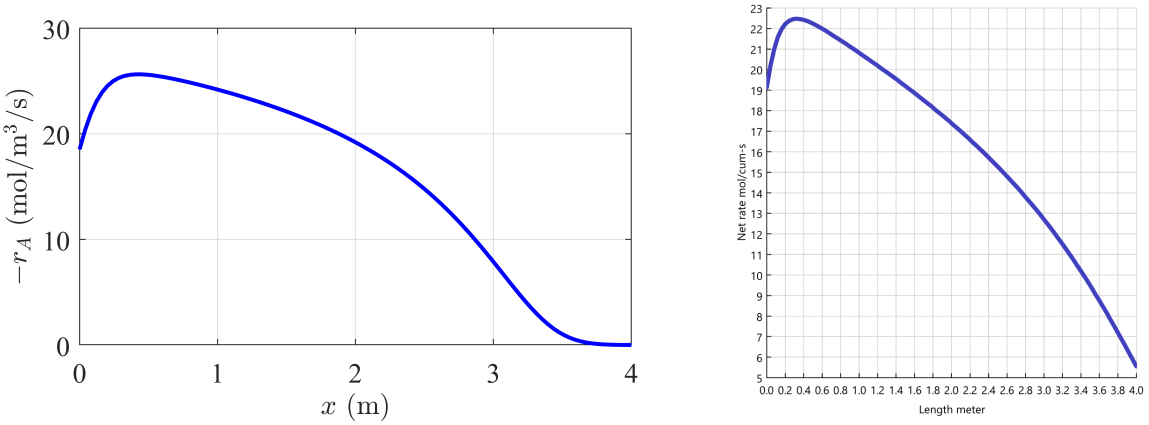

Figure 4: [Left] MATLAB steady reaction rate profile in PFR ; [Right] Aspen Plus steady reaction rate profile in PFR

Qualitatively, the general shape of the solution is the same between both cases, but there are some quantitative differences upon closer inspection. The mole fractions between both cases are very similar, but the MATLAB solver predicts that the reaction goes to completion while the Aspen solution has an outlet acetone mole fraction of about 0.02. This is likely due to the difference in the temperature profiles since the MATLAB solution generally remains slightly hotter than the Aspen solution. This increases the reaction rate and causes MATLAB solution to go to completion. The MATLAB solution predicts an outlet temperature of about 1130 K while Aspen predicts about 1095 K. This major difference party stems from difference in thermodynamics as the MATLAB solver assumes an ideal gas approximation while the Aspen solver uses the Redlich-Kwong EOS. Additionally, Aspen calculates the pressure drop differently than the MATLAB model, leading to a much larger pressure drop compared to the MATLAB model. This larger pressure drop increases the velocity, decreases the residence time, and thus drives the conversion away from 1. In total, the two steady state solutions are comparable and differ slightly due to modeling differences. Therefore, it is verified that the dynamic solver recovers the correct steady solution and can be reasonably used in further explorations.

Dynamic Simulation - No Controller

To test the dynamic solver, the flue gas will remain at a constant 1150 K value while the acetone enters the reactor at $t = 0$ s with a temperature of 1000 K. All parameters will remain as shown in Table 3.

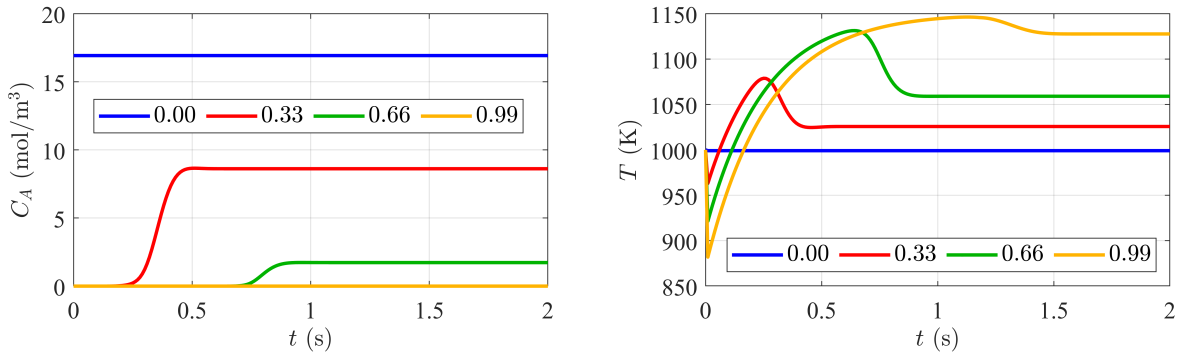

Figure 5: Dynamic profiles of specific points along the PFR, the legend denotes the dimensionless position along the reactor; $U_0 = 4$ m/s; [Left] Acetone concentration; [Right] Reactor temperature

The concentration plot has the expected result of decreasing along the axial distance of the reactor, with the concentration dropping to 0 at the exit, recovering the steady state result shown in the previous section. The dynamic concentration profiles appear almost like higher order linear responses, with a slight S-shape during the rise to the new steady state and a considerable amount of dead time due to the fluid transport. This can be expected since the concentration equation is mostly linear, with only a small nonlinearity given by the Arrhenius term.

The temperature profiles are more interesting as there is a strong interaction between the reactor and heating fluid temperatures. Initially, the temperature at each point starts at its initial value and then increases rapidly due the effect of the heat exchanger. This rapid response is because the reactor is initially filled with an inert (nitrogen) which has a lower heat capacity than acetone, meaning that it takes less energy to heat up. Therefore, when the acetone starts to flow down the reactor, the temperature drops since the acetone and reaction products require more energy to maintain at the same temperature. Additionally, the reaction is endothermic, so a large temperature drop is expected near the entrance of the reactor, where the reaction is still taking place. Conversely, the temperature drop is much lower at the exit, where the reaction is essentially complete and thus consumes little energy. To better visualize how the concentration front travels, consider the following plots of the concentration and temperature in the $z - t$ plane.

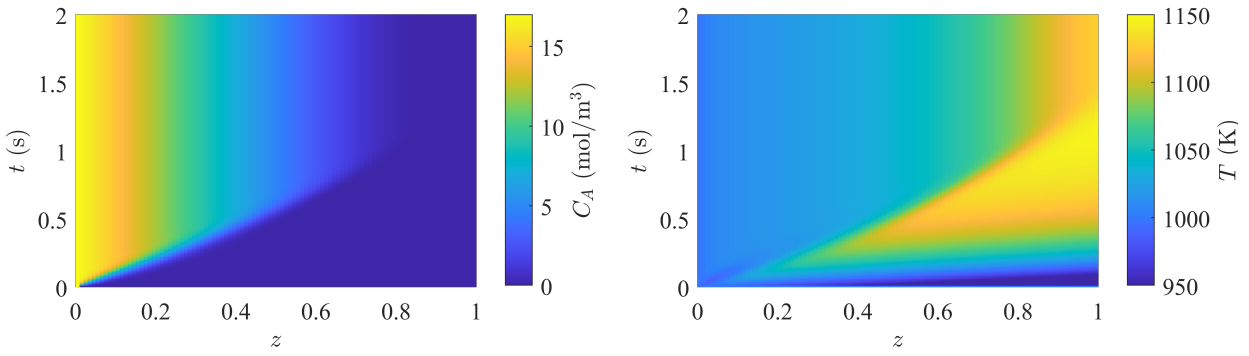

Figure 6: $z - t$ plane of step input to inlet concentration; $U_0 = 4$ m/s; [Left] Acetone concentration; [Right] Reactor temperature

Visually, it is clear how the step input (shock wave) travels along a nearly straight line in the plane. Physically, the slope of this line is the velocity at which the step input travels down the reactor. The slope of the line should be about 4 m/s since that is the inlet velocity and the velocity change is minor. This can be visually confirmed from the plot as when $z = 0.5$, this corresponds to a distance of 2 meters since the total length of the reactor is 4 meters. The corresponding time when the shock hits is about 0.5 seconds. Therefore, dividing the distance by the shock time gives an approximate shock velocity of 4 m/s, as expected. This validates that the simulation captures the correct time scales. The temperature plane follows a similar pattern with a shock velocity of about 4 m/s, but there is noticeable rise in the temperature near the exit of the reactor ($z = 1$). This is again because the reaction is nearly complete there and thus consumes little energy, allowing a higher steady state temperature.

In total, for the given velocity, the reactor is oversized since the acetone concentration drops to 0 inside the reactor. Thus, the velocity should be increased to reduce the residence time and allow for a smaller conversion, but a higher capacity. This would allow for the full length of reactor to be used for reaction. Trying a velocity of 8 m/s yields the following results.

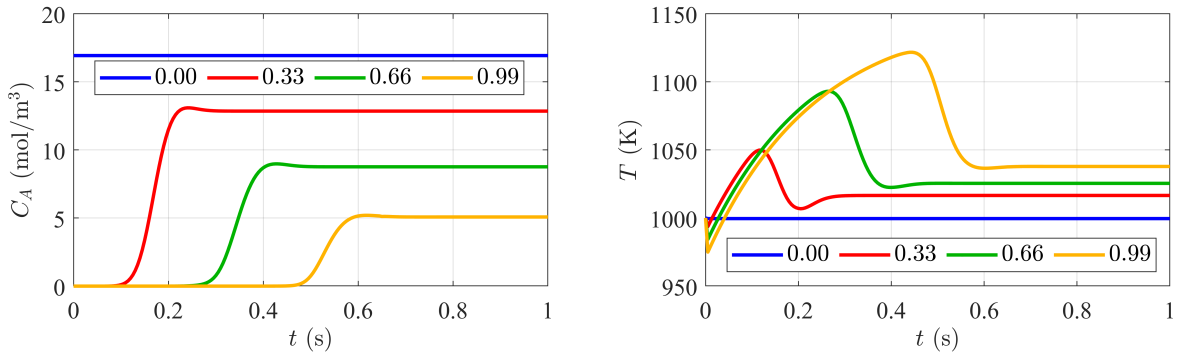

Figure 7: Dynamic profiles of specific points along the PFR, the legend denotes the dimensionless position along the reactor; $U_0 = 8$ m/s; [Left] Acetone concentration; [Right] Reactor temperature

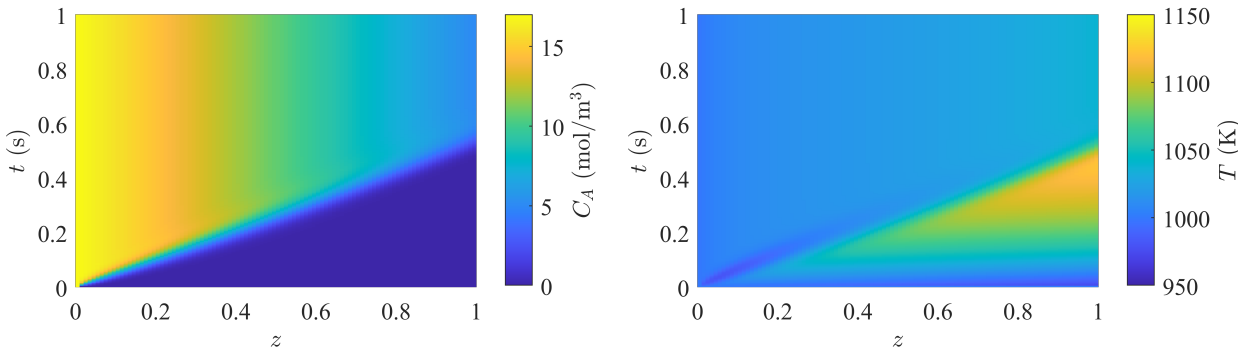

Figure 8: $z-t$ plane of step input to inlet concentration; $U_0 = 8$ m/s; [Left] Acetone concentration; [Right] Reactor temperature

Most of the trends discussed previously are maintained in the new figures. The outlet concentration is about 5 mol/m^3, which confirms that the higher velocity reduces the conversion. As a check for the dynamics, the shock front travels across the reactor (4 m) in about 0.5 seconds, which gives a velocity of 8 m/s , confirming that the correct time scales appear for the new flow rate.

The higher molar flow of the acetone also causes the temperature to drop more significantly when the concentration shock wave appears. The temperature drop exceeds 50 K for $z > 0.66$. This is because the reaction does not go to completion, meaning all of the heat exchanger energy is being used to drive the reaction rather than increasing the temperature of the fluid. Therefore, the temperature profile maintains a sharp shock front along the entire reactor, unlike that $U_0 = 4$ m/s case. A slight overshoot can be seen when the shock front appears, causing the temperature to dip below the new steady state initially. This is likely not physical and is a byproduct of the minmod flux limiter which allows for a slight amount of numerical diffusion. This excess diffusion causes a slight amount of feedback between the concentration and temperature fields and results in the overshoot seen in both profiles.

Further optimization of the reactor flow rate and conversion can be carried out with the steady state solutions. However, this is beyond the dynamics of the PFR, which is the primary objective of this section.

Dynamic Simulation With Control

The proposed control law was implemented in the code, but it does not work as intended as it is hard to shape the dynamic response by manipulating the controller gains. This is because the control objective is hard to define, since it is trying to control an integral-averaged error by manipulating the heating fluid rate. This average error has an unintuitive physical meaning and defining a 'set point' or other common control terminology is not straightforward. Again, this is one of the main drawbacks of countercurrent/cocurrent heating jackets for PFR's. In practice, an empirical model would be developed for the specific reactor and may use alternative controlled and manipulated variables.

Despite this, some initial results are still shown in the following section for controller gains of $K_c = 1000$ and $\lambda = 1$ and an inlet velocity of $U_0 = 8$ m/s.

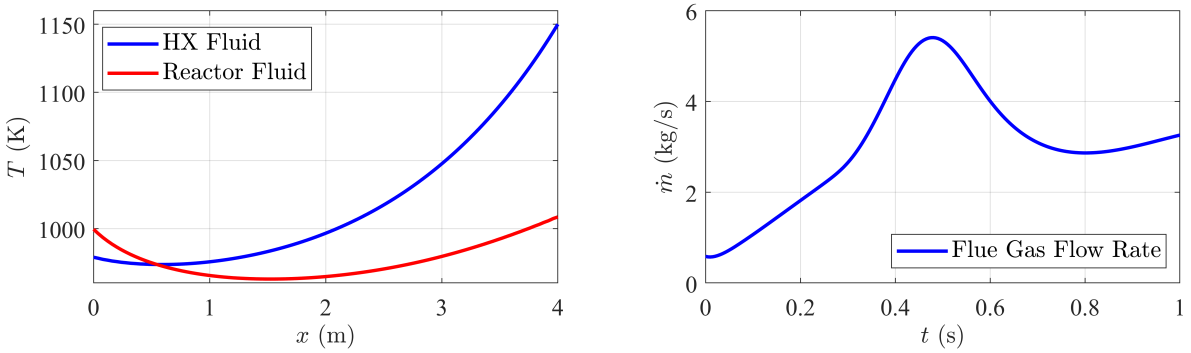

Figure 9: [Left] Steady state heat exchanger profiles for PFR, $U_0 = 8$ m/s; [Right] Dynamic profile of flue gas flow rate with control, $U_0 = 8$ m/s

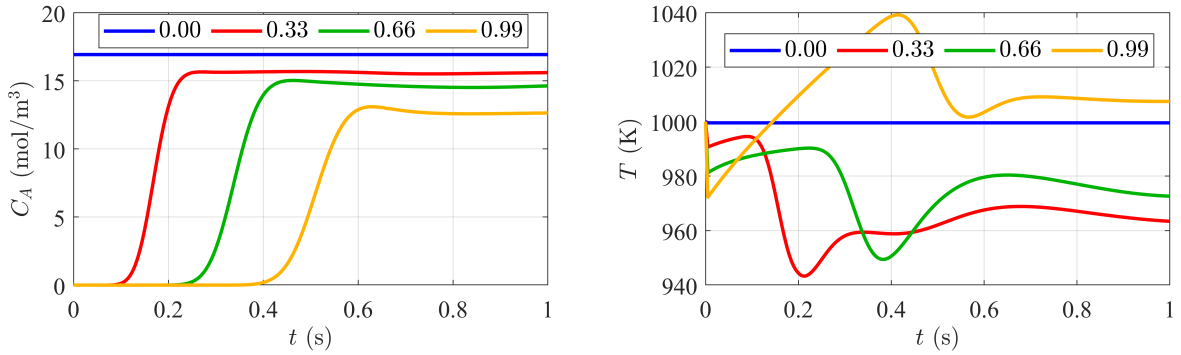

Figure 10: Dynamic profiles of specific points along the PFR, the legend denotes the dimensionless position along the reactor; $U_0 = 8$ m/s; [Left] Acetone concentration; [Right] Reactor temperature

The steady heat exchanger profile exhibits a considerable amount of temperature crossover, with the heating fluid being colder than the reactor fluid at the reactor entrance. This is the trade-off for the controller trying to maintain all points in the reactor near 1000 K. Further studies may wish to vary the controller gains to limit or eliminate this crossover.

The concentration profile shows a much higher outlet concentration of almost 12 mol/m^3 compared to 5 mol/m^3 from the previous section. This is logical because the heat exchanger fluid now drops below 1150 K throughout the reactor while the previous results had a constant heat exchange temperature of 1150 K. This lower temperature slows the reaction and causes the higher outlet acetone concentration. Accordingly, the temperature field is generally lower than the open loop response due to the decreasing heating fluid temperature. The temperature dynamics closely follow the flow rate of the flue gas, as when the flue gas flow peaks at about 0.5 seconds, the temperature profiles near the exit of the reactor

($z = 0.66,\ 0.99$) respond accordingly. For $z = 0.99$, the temperature decreases after $t = 0.5$ s because there is less heating fluid after to warm the end of the reactor. Additionally, the concentration shock wave reaches $z = 0.99$ after $t = 0.5$ s, causing the temperature drop. As the reactor approaches a steady state, the heating flow approaches a steady value of about 3.1 kg/s, causing the temperature profiles to settle out respectively.

Conclusion

In total, a transient model of a plug flow reactor with a countercurrent heat exchanger has been developed and explored. Initial results display reasonable time scales for the open and closed loop responses, but these results have not been fully validated against experimental or other computational work. Further studies should aim to validate the dynamic model by using COMSOL or Aspen Dynamic modeler and ensure the open loop responses match with the MATLAB simulation. Afterwards, the controller model should be improved have a more intuitive interpretation of the controller gains and find methods to select reasonable values that allow the user to have more control over the shape of the closed loop response.

Future work may extend the model to a packed bed reactor, which is much more realistic since gas phase reactions are rarely carried out without a catalyst. Additionally, there are often competing reactions which would imply that a transport equation has to be solved for each species instead of solving for the extent of reaction. Gas phase reactions are also usually run under high pressures where the ideal gas approximation fails. Thus, future goals could implement more detailed thermodynamics with a better EOS and even fugacity models to better capture the interaction between multiple gas species.

References

[1] Fogler, H.S., *Essentials of Chemical Reaction Engineering*. 2nd Ed., Pearson Education Inc., 2018.

[2] *Non-Isothermal Plug Flow Reactor*. COMSOL Multiphysics. https://www.comsol.com/model/nonisothermal-plug-flow-reactor-1404

[3] Heng, P.V., *Notes on Transport Phenomena*. https://github.com/pheng044/Transport_Phenomena

[4] Greenshields, C.J., Weller, H.G., *Notes on Computational Fluid Dynamics: General Principles*. CFD Direct Limited, 2022.

[5] Mcbride, B., Zehe, M., Gordon, S., *NASA Glenn Coefficients for Calculating Thermodynamic Properties of Individual Species*. 2002.

[6] Langtangen, H.P., *Solving Non-Linear ODE and PDE Problems*. Department of Informatics, University of Oslo, 2016.

[7] https://mooseframework.inl.gov/source/systems/NonlinearSystem.html#JFNK

[8] https://www.mathworks.com/help/matlab/ref/spdiags.html

[9] https://www.mathworks.com/help/optim/ug/fsolve.html

[10] Leveque, R. J., *Finite Volume Methods for Hyperbolic Problems*; Cambridge Univ. Press: Cambridge, 2011.

[11] Christofides, P. D.; Prodromos Daoutidis. Feedback Control of Hyperbolic PDE Systems. AIChE Journal 1996, 42 (11), 3063–3086. https://doi.org/10.1002/aic.690421108.